Cancer of the Head and Neck

15

Azusa Hasegawa

Abstract

Carbon-ion radiotherapy, with its powerful biological effects, provides excellent therapeutic efficacy for patients with radioresistant tumors. By focusing the irradiation beam on the target lesion, this approach guarantees a low probability of damage to critical organs (e.g., the brain, spinal cord, eyes, and optic nerves) in the immediate vicinity of the target tumor. With regard to tumors in the head and neck region, carbon-ion radiotherapy is indicated for the treatment of adenoid cystic carcinomas, adenocarcinomas, and malignant mucosal melanomas in the oral and maxillofacial area. The safety and efficacy of this therapy have been established. Certain groups of radioresistant tumors are not indicated for surgical resection because of possible surgery-induced injury to critical organs, and these tumors raise a significant clinical concern because of the paucity of effective treatment options. Carbon-ion radiotherapy will represent a definitive treatment for these malignancies.

Keywords

Adenoid cystic carcinoma • Carbon ions • Head and neck cancer • Mucosal malignant melanoma • Radiotherapy

15.1 Introduction

It is often difficult to completely eradicate malignant tumors in the head and neck region by surgery alone, owing to the location of these tumors or progression. Radiotherapy is, in most cases, the first-line treatment of choice for such tumors. In the head and neck region, however, various types of non-squamous cell tumors that are not sensitive to photon radiotherapy (X- and γ-rays) develop. Dose restrictions for the critical organs located in the proximity of the target lesion (e.g., the brain, brain stem, spinal cord, eyeballs, and optic nerves) limit the administration of sufficient therapeutic radiation doses. For these reasons, a considerable proportion of cases of non-squamous cell neoplasms of the head and neck region are diagnosed as intractable, resulting in poor local control rates [1–7].

In June 1994, the National Institute of Radiological Sciences (NIRS) initiated a clinical trial on heavy charged particle therapy for malignant head and neck tumors; for these tumors, the radiation oncologist can clearly visualize reactions in the adjacent skin and mucous membrane that serve as dose-limiting factors. Carbon ions exhibit excellent dose localization attributable to their physical characteristics, commonly known as the Bragg peak, in addition to beneficial biological effectiveness [8]. Because of these features, carbon-ion radiotherapy has been expected to serve as an effective tool for the treatment of radioresistant tumors, and its safety and effectiveness have been established for tumors of various sites [9–11].

A clinical trial of carbon-ion radiotherapy for malignant head and neck tumors was conducted under the "Phase I/II Clinical Trial (Protocol 9301) on Heavy Particle Radiotherapy for Malignant Head-and-Neck Tumors," which was initiated

A. Hasegawa (✉)
Research Center Hospital for Charged Particle Therapy, National Institute of Radiological Sciences, 4-9-1 Anagawa, Inage-ku, Chiba 263-8555, Japan
e-mail: azusa@nirs.go.jp

H. Tsujii et al. (eds.), *Carbon-Ion Radiotherapy: Principles, Practices, and Treatment Planning*,
DOI 10.1007/978-4-431-54457-9_15,

in June 1994 by way of a dose escalation study using 18 fractions over 6 weeks. This trial was followed by another dose escalation study that commenced in April 1996 under the title of "Phase I/II Clinical Trial (Protocol 9504) on Heavy Particle Radiotherapy for Malignant Head-and-Neck Tumors," which used 16 fractions over 4 weeks. On the basis of the outcome of these two studies [12], the "Phase II Clinical Trial on Heavy Particle Radiotherapy for Malignant Head-and-Neck Tumors (Protocol 9602)" was initiated in April 1997, using 57.6 or 64.0 GyE in 16 fractions over 4 weeks. The dose level to be used depends on the tumor size and possibility of sparing critical organs.

15.2 Significance of Carbon-Ion Radiotherapy

Non-squamous cell, locally advanced tumors are generally considered poor candidates for photon radiotherapy and/or chemotherapy; however, carbon-ion radiotherapy (C-ion RT) showed excellent therapeutic effectiveness for these types of tumors. C-ion RT will prove beneficial as first-line local treatment for advanced tumors that are not indicated for surgery.

High-linear energy transfer charged particles such as carbon ions have excellent dose-localizing properties, and this can potentiality cause severe damage to the tumor while minimizing the effect of the treatment on normal tissue. When the tumor is located close to critical organs, the clinical target volume (CTV) is delineated, with efforts made to spare these organs.

15.3 General Management of Radiation Technique

Target contouring is performed by employing multimodality imaging and image fusions. Each patient is studied using simulation computed tomography (CT), gadolinium-enhanced magnetic resonance imaging (MRI), and 11C-methionine positron emission tomography (MET-PET). The gross tumor volume (GTV) encompasses the gadolinium-enhanced area and the area with high methionine uptake.

A shrinking-field technique is employed: the larger CTV1 receives the first 9 or 10 fractions and the reduced CTV2 receives the remaining 6 or 7 fractions. CTV1 encompasses a 10- to 15-mm uniform margin around the GTV. CTV1 can be reduced if anatomical barriers are present (e.g., for an extracranial tumor with no evidence of skull invasion, the brain is excluded from CTV1). CTV1 is usually enlarged to cover any suspected areas. In mucosal malignant melanoma (MMM), if the GTV involves part of a mucosal cavity, the entire cavity is usually included in CTV1. In adenoid cystic carcinoma (ACC), if the GTV involves part of a cranial nerve, the entire nerve is included in CTV1 up to the skull base. CTV2 encompasses a 5-mm uniform margin around GTV. It can be reduced to spare the skin, optic nerve, or other critical organs. In particular, when the eyeball or optic nerve is involved in the high-dose area, treatment planning is performed to spare the contralateral optic nerve and chiasm according to our previous dose criteria [13, 14]. Efforts are being made to decrease untoward adverse reactions by clinically applying the results of these studies.

15.3.1 Skin Reaction

Late skin reaction is an adverse effect that, depending on the severity, could significantly impair the quality of life. Extensive efforts are being made to minimize the risk of severe skin toxicity, including the use of multi-portal irradiation. A trade-off between adequate target coverage (local control) and skin sparing may be necessary, for which a 3-dimensional surface dose distribution of the skin has been used as a powerful tool to evaluate treatment plans. In our experience, marginal recurrence due to overgenerous skin sparing is a rare event (<5 %).

15.3.2 Brain Toxicity

Brain necrosis is a side effect often encountered after high-dose radiotherapy. Vascular injury, direct damage to glial cells, changes in the fibrinolytic enzyme system, and immune response are all relevant pathophysiological mechanisms, but their relative role is not yet completely clear. Radiation-induced brain necrosis is a serious complication that usually shows a progressive course, threatening the patient's life.

In C-ion RT, brain necrosis may develop in the region where the tumor was present and a high dose was administered. Necrosis is usually locally confined and asymptomatic. A cystic lesion may develop, which sometimes needs to be managed by surgical removal. Treatment planning should be performed to irradiate the smallest possible amount of normal brain tissue.

15.3.3 Optic Nerve Complications

Optic nerve irradiation can cause partial or complete visual loss, in particular when the optic nerve is involved or encased by the tumor. The tolerance dose for whole-organ irradiation with photons using conventional fractionation is well known (TD5/5 = 50 Gy; TD50/5 = 65 Gy). The tolerance of optic nerves to C-ion RT has been previously reported. Dose of 20 % volume of the optic nerve (D_{20}) has been shown to be

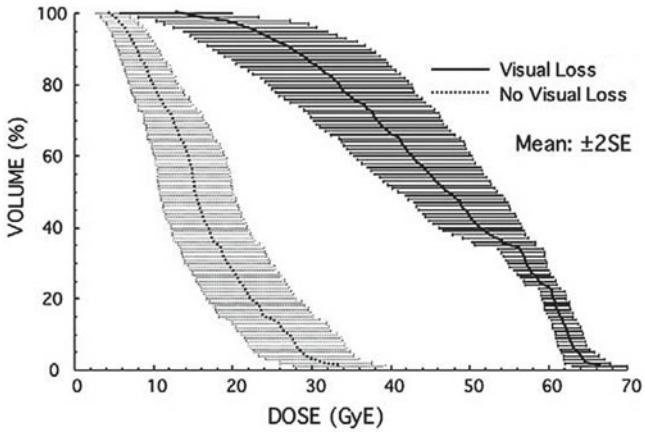

Fig. 15.1 DVH analysis was performed to compare optic nerves that did and did not develop toxicity

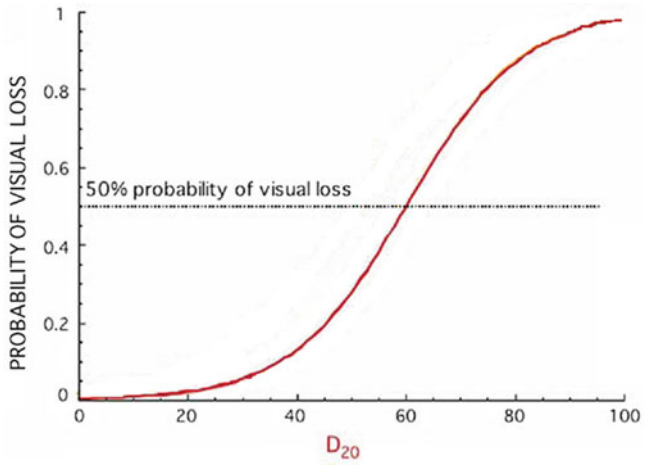

Fig. 15.2 Probability of visual loss as a function of D_{20} was calculated according to an integral logistic model

the most statistically significant predictor of toxicity. The incidence of visual loss has been 58 % when a maximum dose (D_{max}) in excess of 55 GyE and 48 % when a D_{20} in excess of 40 GyE was delivered (Figs. 15.1 and 15.2).

Every effort should be made to spare the uninvolved optic nerve so that bilateral visual acuity loss can be avoided. Dose constraints at NIRS have been previously published, in which the most relevant parameter is D_{20}. Preservation of visual acuity at a risk of <5 % can be achieved if D_{20} is maintained lower than 30 GyE. It is important to evaluate the risk on the basis of the whole nerve dose-volume histogram (DVH) and not only the specific dose or volume.

15.3.3.1 Optic Nerve Sparing

The GTV (Fig. 15.3, dark orange line) is contoured according to contrast MRI, CT, and MET-PET images, and image fusion is routinely employed. A shrinking-field technique is employed in head and neck cancer. The larger CTV1 (Fig. 15.3, light orange line) receives the first 9 fractions and the smaller CTV2 receives the last 7 fractions. Addition of uniform geometric margins around the GTV would result in CTV1 and CTV2, which were drawn similarly for avoidance of irradiation to the right optic nerves (Fig. 15.3, blue contours). Irradiation of the left optic nerve was unavoidable (Fig. 15.4).

This 76-year-old male patient with ACC was treated in December 2008. The prescribed dose was 64 GyE in 16 fractions over 4 weeks. At 37 months after C-ion RT, the patient is alive, with local control and preservation of visual acuity in both eyes.

15.3.4 Osteonecrosis

In radiation therapy, blood supply to the bone may be inhibited at the microscopic level. In particular, if the bone is destroyed by the tumor and irradiated with high-dose carbon ions or photons, the bone may undergo necrotic changes and subsequent infection may occur. Osteonecrosis caused by both tumor involvement and irradiation is extremely difficult to treat and can cause severe pain. Surgical resection of necrotic bone (sequestrectomy) may be necessary for pain control. The jawbone is also more prone to radiation-induced necrosis because of exposure to the oral bacterial load.

When the bone infiltrated by the tumor is irradiated at a high dose (for instance, in sarcoma cases), the risk of bone necrosis may be unavoidable. Oral care with weekly irrigation has the potential of lowering this risk. When bone necrosis develops, it is important to administer conservative treatment first, with systemic antibiotics, analgesics, and local antiseptic agents. Surgical resection may be necessary if the patient experiences severe pain. Close cooperation between the radiation oncologist and the oral and maxillofacial surgeon is required, and treatment planning should be optimized to allow future implant surgery (for instance, sparing zeugmatic processes whenever possible).

15.4 Results of Therapy

Between April 1997 and August 2012, a total of 438 cases were treated using 57.6 or 64.0 GyE. Histologically, 175 patients had ACC, 102 had MMM, 50 had adenocarcinoma, and the others had different diagnoses. With regard to the tumor site studied, the paranasal sinus was studied in 119 cases, the nasal cavity in 81, the major salivary gland in 59, the oral cavity in 54, the pharynx in 51, and other sites in the remaining cases. Almost all patients (74 %) had inoperable tumors.

The 5-year local control rates according to major histological types in our institution were as follows: 81 % for

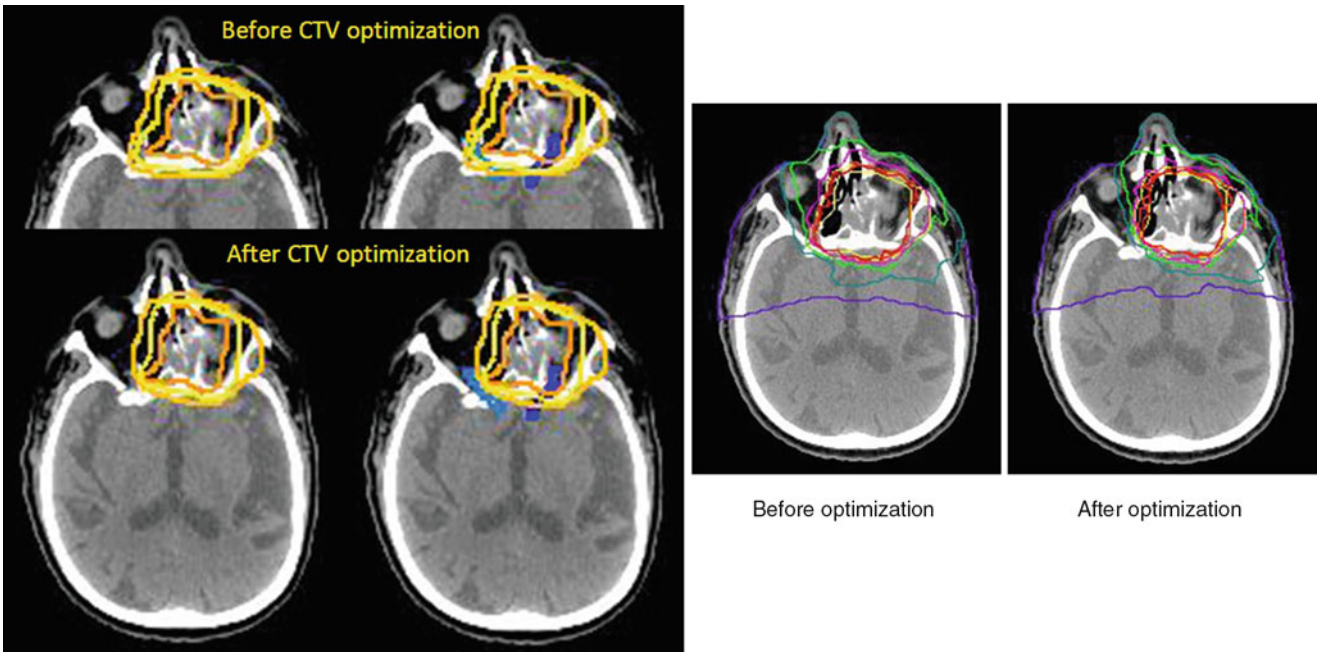

Fig. 15.3 Before CTV optimization, both optic nerves were included in the high-dose area. After CTV optimization, good sparing of the right optic nerve was achieved. Isodose level: *red* = 96 %; *orange* = 90 %; *magenta* = 70 %; *green* = 50 %; *cyan* = 30 %; *purple* = 10 %. Contour: *dark orange* = gross tumor volume, *light orange* = large clinical target volume, *yellow* = small clinical target volume

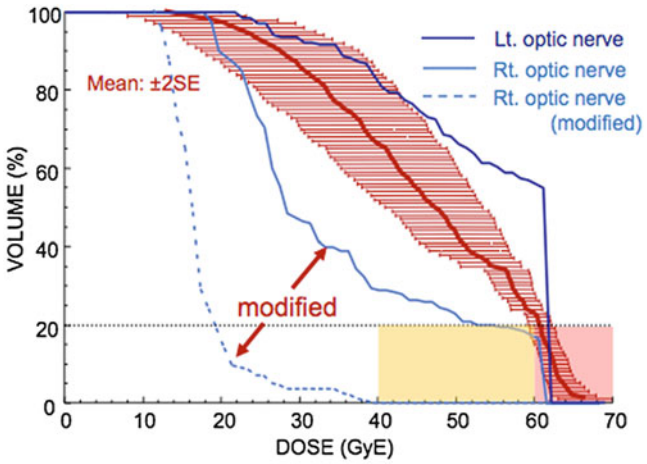

Fig. 15.4 Probability of visual loss: *red zone* 58 %, *yellow* 30 %, *pink* 50 %. Relatively small changes in CTV can produce a dramatic effect on the optic nerve DVH

adenocarcinomas, 74 % for ACCs, and 79 % for MMMs. With regard to the prescribed tumor dose, the 5-year local control rates of ACC were 81 % for the 64 GyE group and 69 % for the 57.6 GyE group. Although this rate did not differ significantly between these groups ($p = 0.0789$), the local control rate for the 64 GyE group tended to be better. However, 14 patients with bone and soft tissue sarcomas in the head and neck region (mostly osteosarcomas) had a poor 5-year local control rate, although a majority of the patients received 64 GyE. Consequently, a new treatment protocol was introduced in April 2001 to apply a total irradiation dose of 70.4 GyE in 16 fractionations over 4 weeks (see Chap. 17), a schedule similar to that used for the treatment of bone and soft tissue sarcomas of the trunk.

Additionally, the 5-year overall survival rates were 57 % for adenocarcinomas, 72 % for ACCs, and 33 % for MMMs. Although the local control facilitated by C-ion RT was promising for MMM, the survival rate was not commensurate with the favorable local control rate because of subsequent regional lymph node or distant metastases. Further to the results of preliminary analysis of this study, a new protocol was introduced in April 2001 for the purpose of prophylactic therapy against distant metastasis, the major cause of death in MMM of the head and neck region (see Chap. 16).

Regarding late radiation morbidities, almost all of the late skin and mucosal reactions were of grade 1 or lower. Less than 5 % of the patients developed grade 2 skin or mucosal reactions. The recorded tumor-related events that needed surgical treatment included encephalitis, sinusitis, otitis media, and maxillary bone necrosis. These events were documented in patients that had been informed before the start of therapy about the possibility of adverse events due to tumor infiltration. Other patients reported no unexpected serious adverse reactions.

15.5 Case Studies

15.5.1 Skin Reaction

15.5.1.1 A Case with Severe Skin Reaction

A 59-year-old man with MMM was treated with C-ion RT in July 1997. A bulky tumor invading the right nasal and paranasal cavity was observed on enhanced MRI (Fig. 15.5). The prescribed dose was 57.6 GyE in 16 fractions over 4 weeks. During the early phase of the dose escalation study, most of the tumors were treated using only two portals from the antero-posterior and lateral directions, with the safety margin being drawn equally around the GTV or CTV. Therefore, when the tumor invaded or was close to the overlying skin, it was also irradiated with the same dose as was administered to the tumor. This treatment was applied in the current case, in which the cheek skin was included for irradiation with high-dose levels, as shown in the Fig. 15.5b.

At 52 months after C-ion RT, the patient showed complete disappearance of the tumor but developed external fistula of the skin (Figs. 15.5c and 15.6-middle) corresponding to the high-dose area (Fig. 15.6-left).

In this case, only two portals were used and no specific plan for sparing the skin was considered at the time. A wide surface of the skin received the full dose. Local control was achieved, but a severe late effect developed corresponding to the high-dose area. Although this patient had received surgery for skin grafting (Fig. 15.6-right), he survived 58 months after C-ion RT and died of intercurrent diseases.

15.5.1.2 A Case with Acceptable Skin Reaction

A 63-year-old woman with MMM of the left nasal and paranasal cavity was treated with C-ion RT from January to February 2007. The prescribed dose was 64.0 GyE in 16 fractions over 4 weeks. In this case, a very tight margin toward the cheek skin was set to reduce the dose to the skin (Fig. 15.7).

Twenty-five months after C-ion RT, the patient is alive without tumor progression. No significant late toxicity is present apart from a right facial nerve deficit, which was already present at diagnosis (Fig. 15.8).

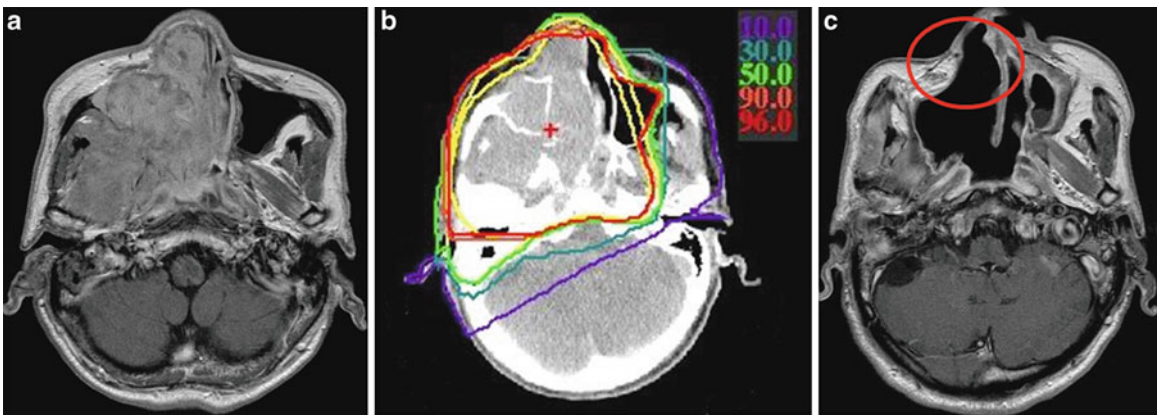

Fig. 15.5 Gadolinium-enhanced T1WI images and isodose distribution. (**a**) Before treatment, (**b**) isodose distribution, (**c**) after treatment. Isodose level: *red* = 96 %; *orange* = 90 %; *green* = 50 %; *cyan* = 30 %; *purple* = 10 %. Contour: *yellow* = clinical target volume

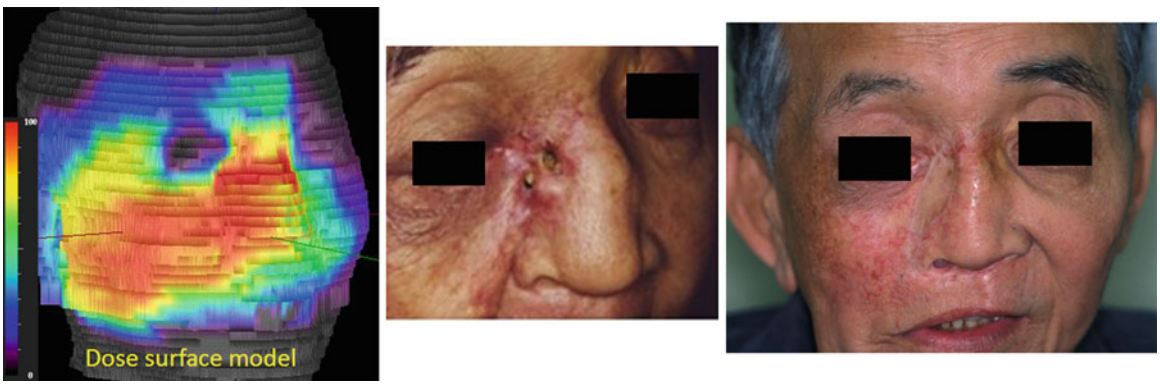

Fig. 15.6 Dose-surface model and skin reaction. The image on the right side is taken after skin grafting

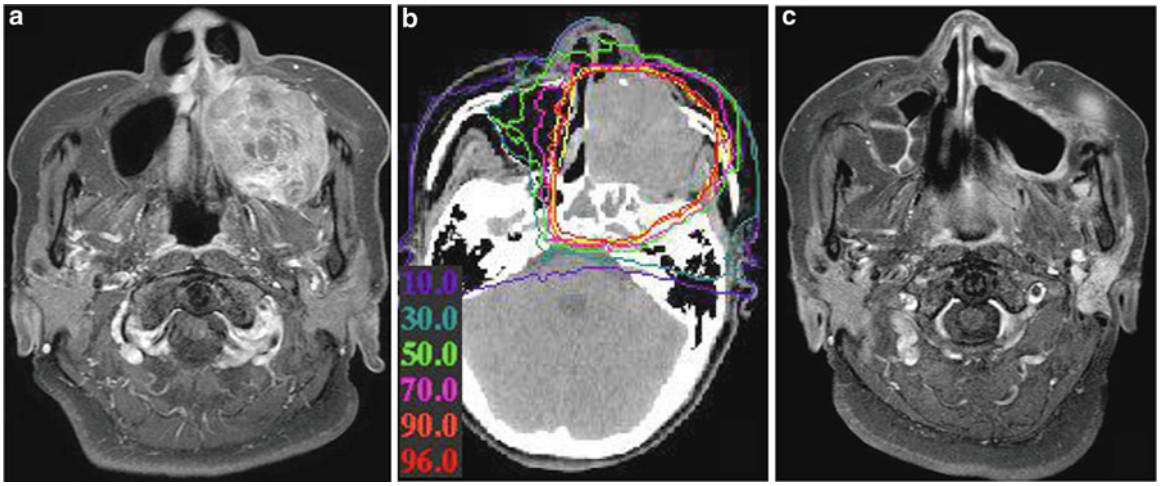

Fig. 15.7 Gadolinium-enhanced T1WI images and isodose distribution. (**a**) Before treatment, (**b**) isodose distribution, (**c**) after treatment

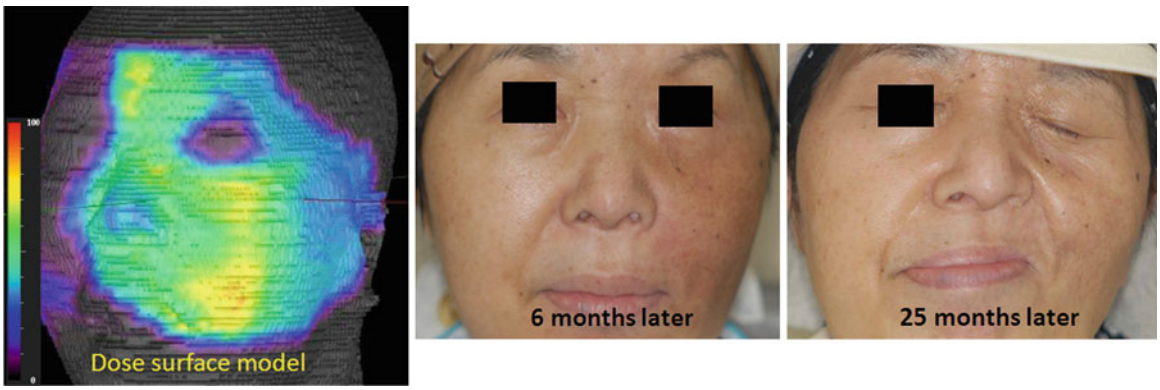

Fig. 15.8 Dose-surface model and skin reaction

15.5.2 Brain Toxicity

15.5.2.1 A Case with Late Grade 2 Reaction

A 54-year-old man with postoperative recurrence of ACC in the palate was treated with C-ion RT in April 2002. The tumor originated from the palate and extended upward to invade the brain. The dose delivered to the CTV was 57.6 GyE in 16 fractions over 4 weeks using three portals (Fig. 15.9). At 22 months after C-ion RT, grade 2 brain reaction (RTOG/EORTC, SOMA LENT) developed and was treated with steroids (Fig. 15.10). All of these lesions were found within the dose level of 70 % or greater of the prescribed dose. At 85 months after C-ion RT, there is no evidence of local recurrence and the patient is asymptomatic, requiring no medication.

15.5.2.2 A Case with Cyst Formation

A 25-year-old man with giant cell tumor was treated with C-ion RT in June 2001 (Fig. 15.11). The tumor appeared to invade the right temporal lobe. The prescribed dose was 57.6 GyE in 16 fractions over 4 weeks using three oblique portals. The brain injury was developed with cystic change in the right temporal lobe. Surgical removal of cystic lesion was performed for severe headache. This patient does not require any medication after surgery. At 8 years after C-ion RT, the patient is alive with no evidence of tumor progression.

15.5.3 Optic Nerve Complications

15.5.3.1 A Case with Visual Loss in the Involved Side

A 71-year-old man with MMM was treated with C-ion RT in November 1998. The tumor occupied the nasal cavity and ethmoidal sinus. Evidence of direct tumor invasion of the left orbit and left optic nerve was noted on enhanced MRI. The tumor was close to the right optic nerve. A total dose of 57.6 GyE was delivered in 16 fractions over 4 weeks using two portals (antero-posterior and left lateral) (Fig. 15.12). A reduced margin was employed in order to avoid irradiation

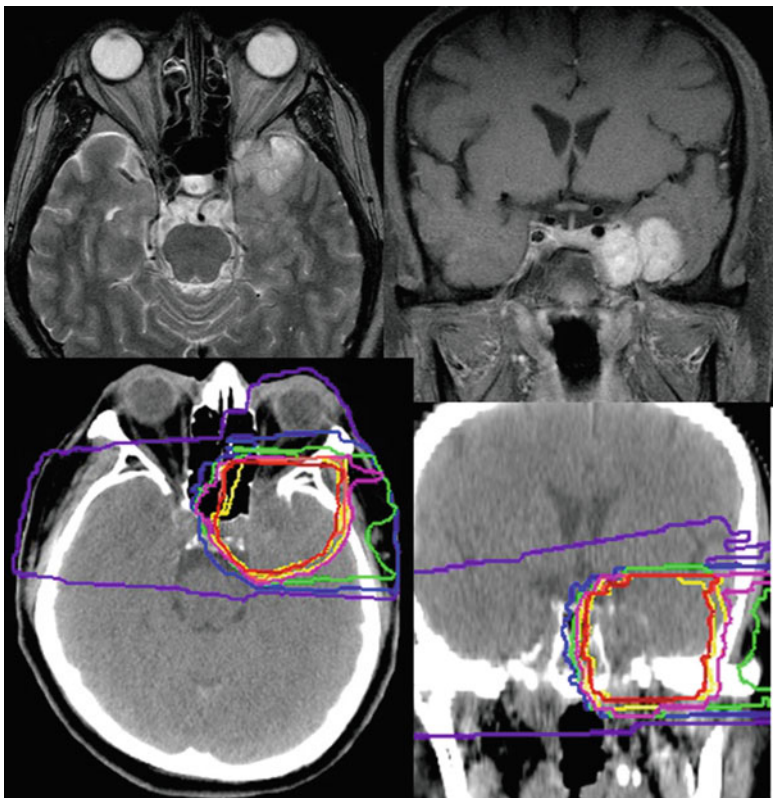

Fig. 15.9 MRIs before treatment and isodose distribution. Isodose level: *red* = 96 %; *orange* = 90 %; *magenta* = 70 %; *green* = 50 %; *cyan* = 30 %; *purple* = 10 %. Contour: *yellow* = clinical target volume

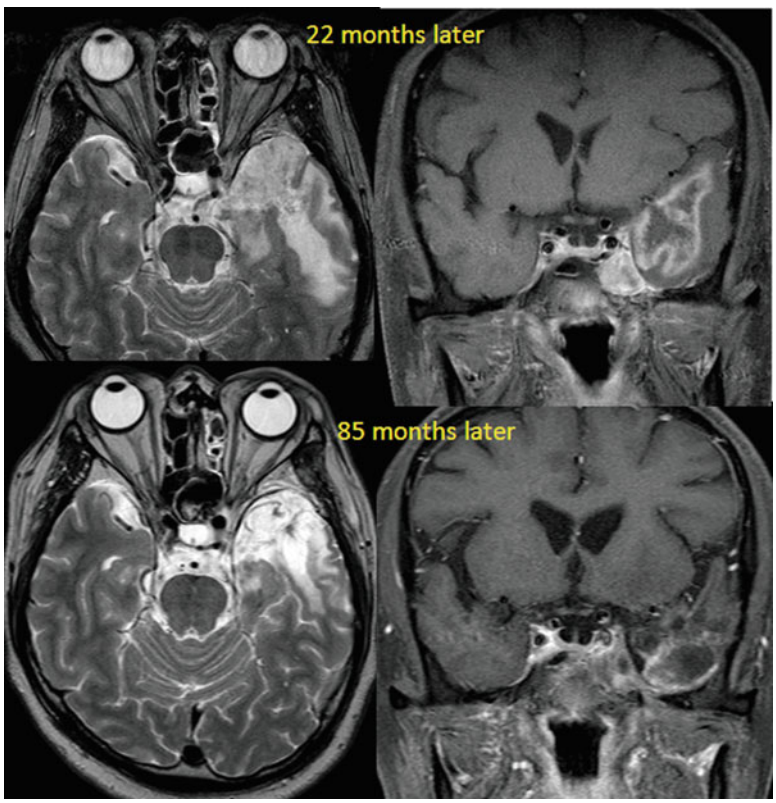

Fig. 15.10 MRIs after treatment

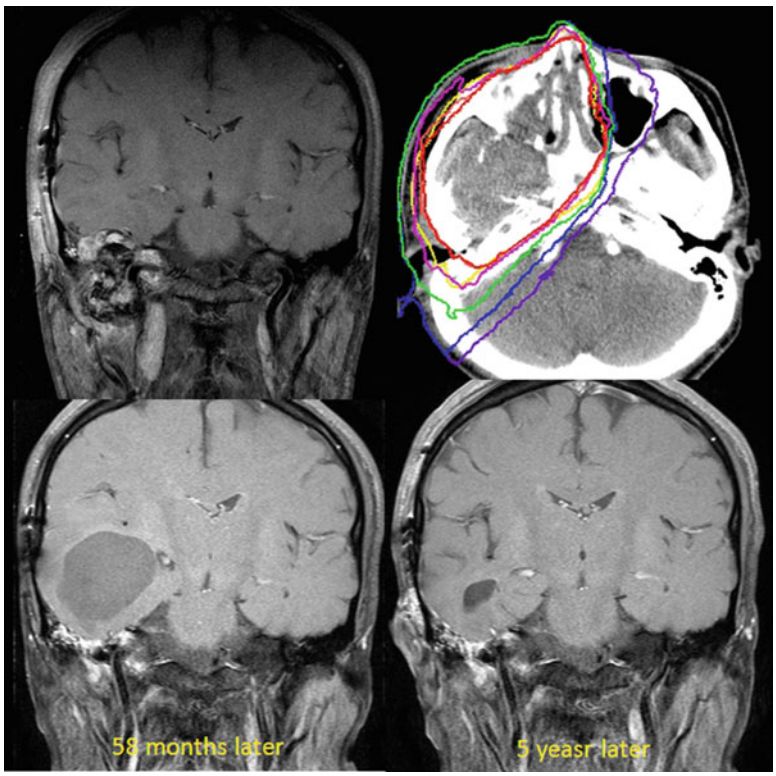

Fig. 15.11 Isodose distribution and MRIs before and after treatment. Isodose level: *red* = 96 %; *orange* = 90 %; *magenta* = 60 %; *green* = 50 %; *cyan* = 30 %; *purple* = 10 %. Contour: *yellow* = clinical target volume

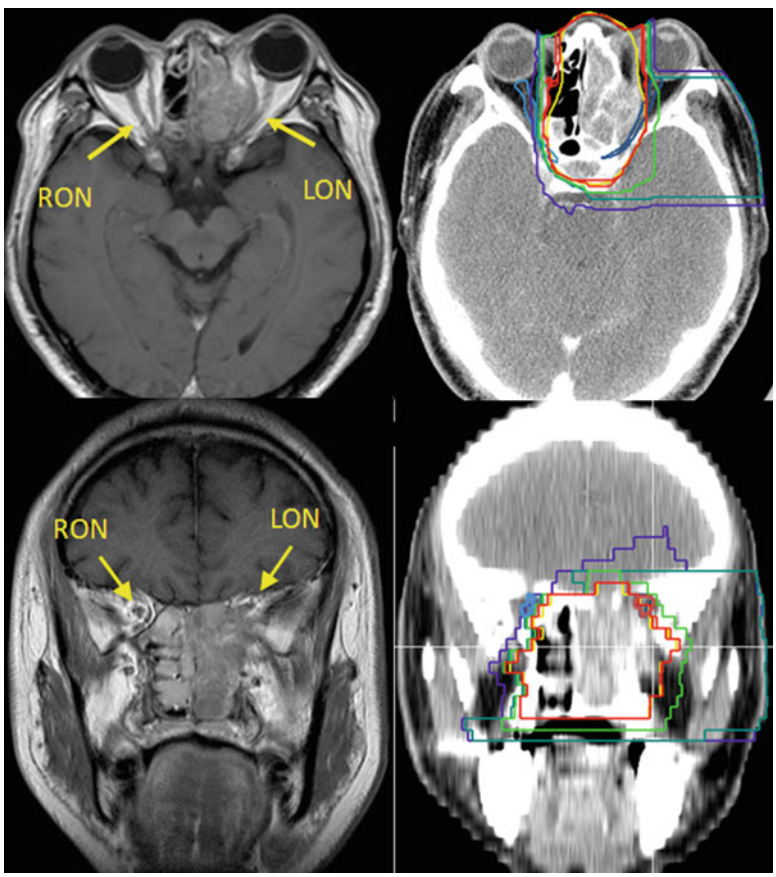

Fig. 15.12 MRIs before treatment and isodose distribution. Isodose level: *red* = 96 %; *orange* = 90 %; *green* = 50 %; *cyan* = 30 %; *purple* = 10 %. Contour: *yellow* = clinical target volume

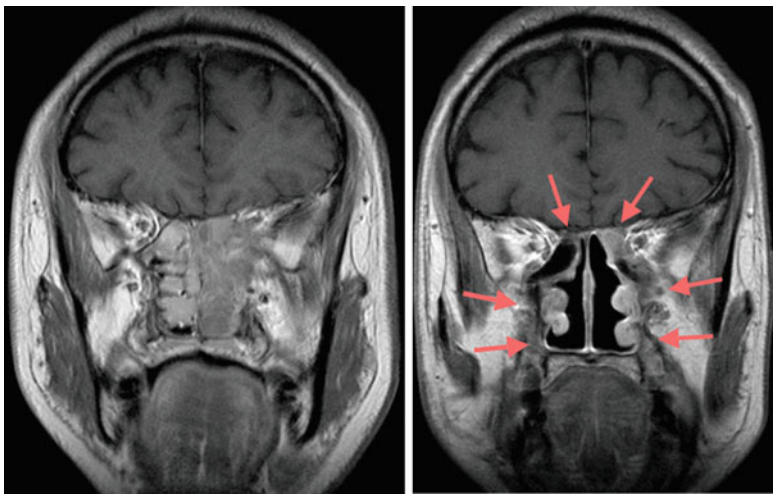

Fig. 15.13 After 22 months, MRI shows complete local response

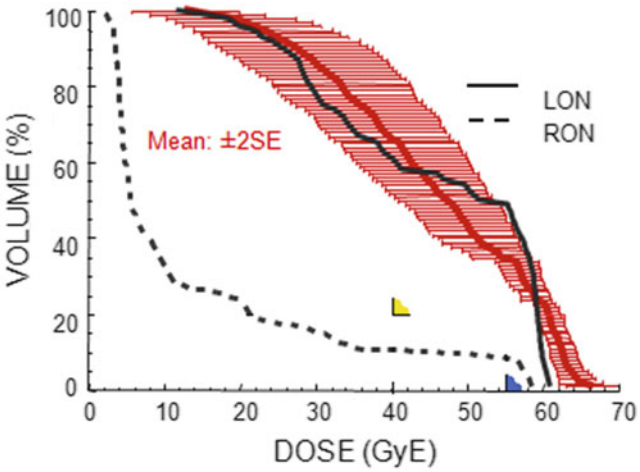

Fig. 15.14 Left optic nerve DVH (*full line*) was in the region that had resulted in visual loss in past experience at NIRS. Right optic nerve DVH (*broken line*) was within acceptable constraints for D_{20} (*yellow triangle*) but slightly above safe levels for D_{max} (*blue triangle*)

of the right optic nerve. Care was taken to avoid the patch line within the optic nerve, although the right optic nerve did receive high-dose irradiation.

The patient was alive without tumor progression for 73 months after C-ion RT (Fig. 15.13). There has been complete visual loss in the left eye, whereas the visual acuity of right eye has remained unchanged (Fig. 15.14) [13].

15.5.4 Osteonecrosis

15.5.4.1 A Case with Osteosarcoma

A 52-year-old woman with maxillary bone osteosarcoma was treated with C-ion RT in June 2004. The bone was partially destroyed by tumor as shown on MRI and CT scans (Fig. 15.15a). The prescribed dose was 70.4 GyE in 16 fractions over 4 weeks using three oblique portals (Fig. 15.15b). Nine months after C-ion RT, the patient developed well-defined bone necrosis. At 14 months after C-ion RT, since the tumor was locally controlled and the necrotic bone was locally limited, surgical resection of necrotic bone was performed for pain control. A denture and palatal prosthesis were successfully applied (Fig. 15.16). At 62 months after C-ion RT, the patient is alive with no evidence of disease.

The bone infiltrated by tumor can easily result in bone necrosis after radiotherapy. After C-ion RT, as bone necrosis is generally limited, it can be surgically resected; thereafter, a denture and palatal prosthesis can be applied in most cases.

15.5.4.2 A Case with Mucosal Malignant Melanoma

A 63-year-old woman with MMM of the left nasal and paranasal cavity was treated with C-ion RT from January 5 to February 1, 2007 (Fig. 15.17). The prescribed dose was 64.0 GyE in 16 fractions over 4 weeks. This is the same patient as in a case with acceptable skin reaction (20.6.1.2). At 25 months after C-ion RT, since the tumor was locally controlled and the necrotic bone was locally limited, surgical resection of necrotic bone was performed for pain control (Fig. 15.18). A denture and palatal prosthesis were successfully applied. At 62 months after C-ion RT, the patient is alive with no evidence of disease.

15.5.5 Recurrence Pattern and Re-Irradiation

Loco-regional recurrence of the tumor is classified as "in-field recurrence" if the lesion recurs within the high-dose volume (planning target volume, PTV), "marginal recurrence" if it recurs on the boundary of the PTV, and "regional recurrence" if the tumor recurs in the region nearby but apart from the PTV. When the shrinking technique is used, it is very difficult to distinguish in-field and marginal recurrence.

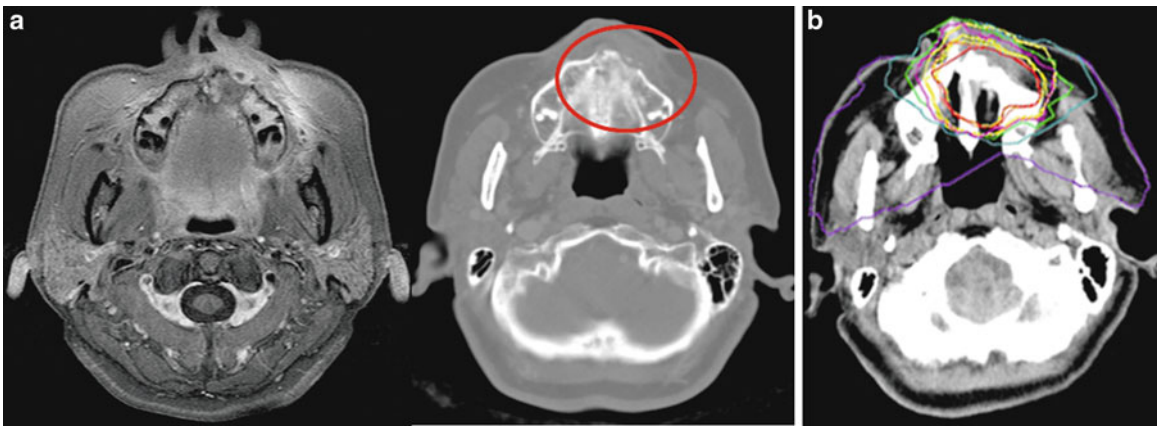

Fig. 15.15 Gadolinium-enhanced T1WI image, CT, and isodose distribution. (**a**) Before treatment, (**b**) isodose distribution. Isodose level: *red* = 96 %; *orange* = 90 %; *magenta* = 60 %; *green* = 50 %; *cyan* = 30 %; *purple* = 10 %. Contour: *yellow* = clinical target volume

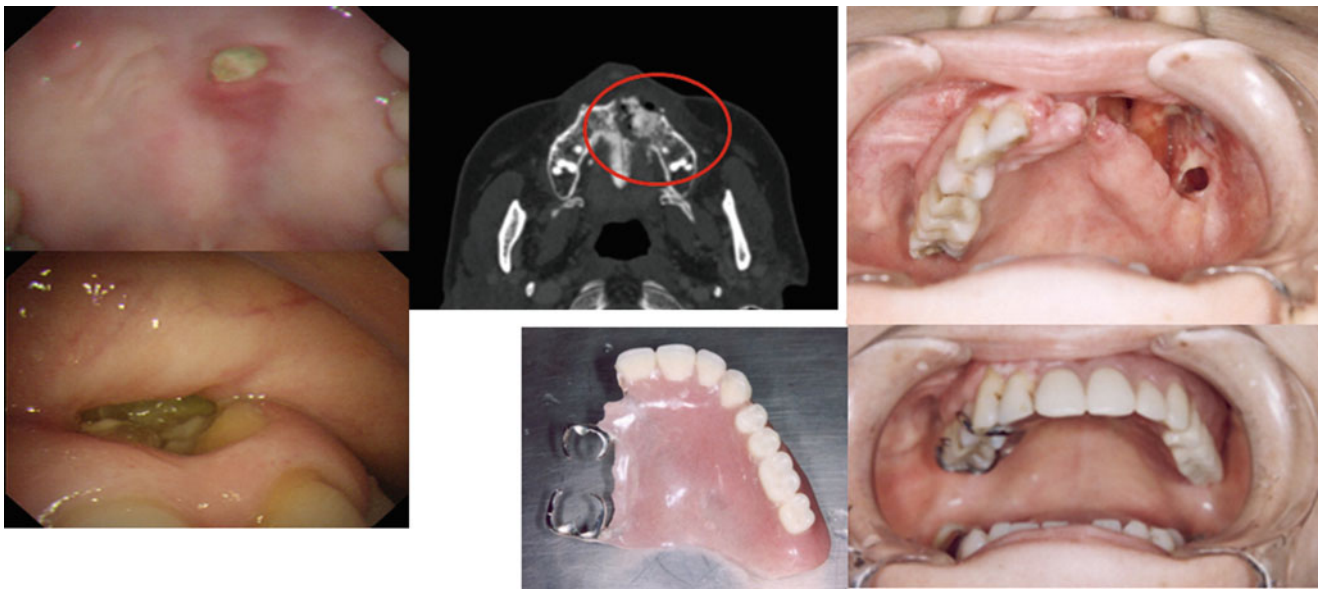

Fig. 15.16 Osteonecrosis after sequestrectomy

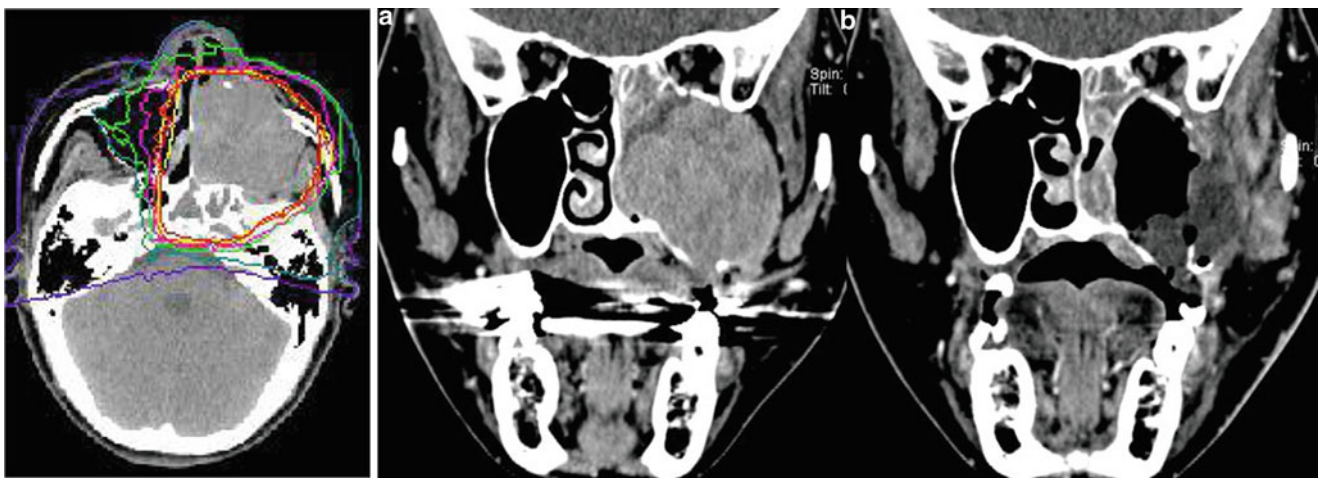

Fig. 15.17 Isodose distribution and CT images. (**a**) Before treatment, (**b**) after treatment. Isodose level: *red* = 96 %; *orange* = 90 %; *magenta* = 70 %; *green* = 50 %; *cyan* = 30 %; *purple* = 10 %. Contour: *yellow* = clinical target volume

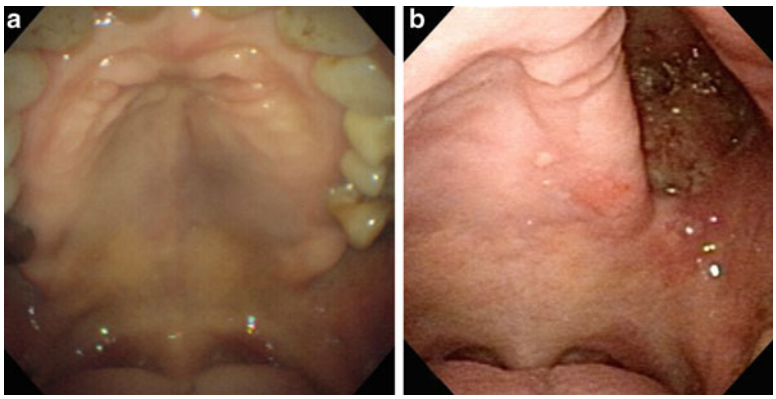

Fig. 15.18 Clinical pictures of the palate. (**a**) Before treatment, (**b**) after treatment and sequestrectomy

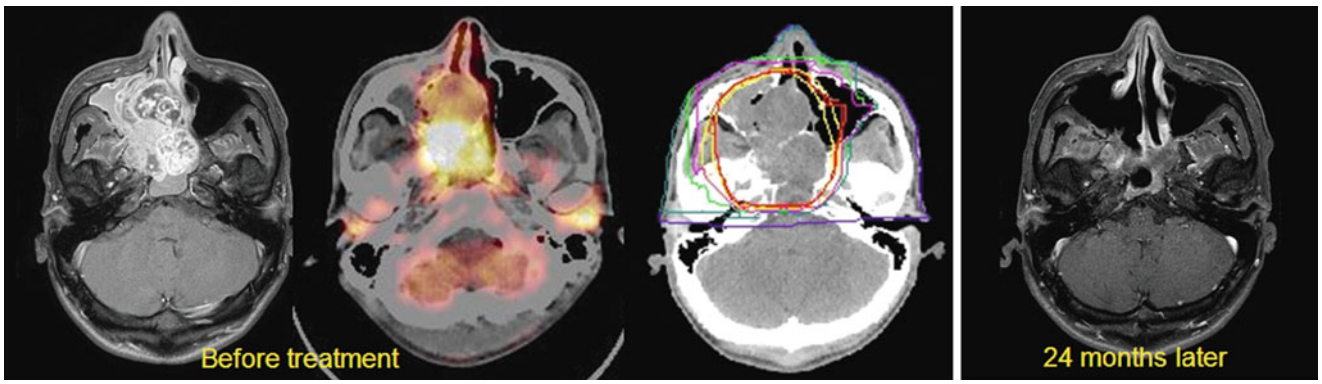

Fig. 15.19 Magnetic resonance and MET-PET images before treatment, isodose distribution, and 24 months later. Isodose level: *red* = 96 %; *orange* = 90 %; *magenta* = 60 %; *green* = 50 %; *cyan* = 30 %; *purple* = 10 %. Contour: *yellow* = clinical target volume

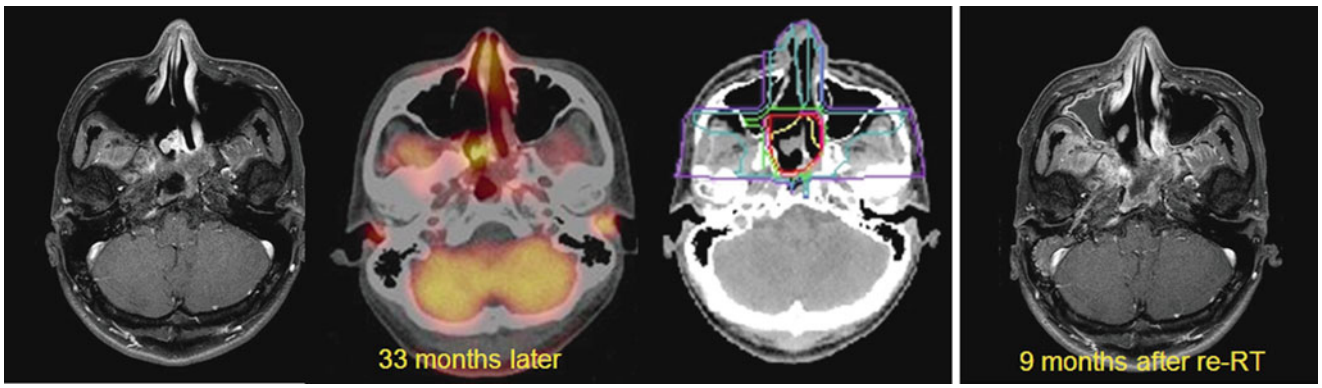

Fig. 15.20 Magnetic resonance and MET-PET images before re-irradiation, isodose distribution, and after re-irradiation. Isodose level: *red* = 96 %; *orange* = 90 %; *magenta* = 70 %; *green* = 50 %; *cyan* = 30 %; *purple* = 10 %. Contour: *yellow* = clinical target volume

Since 2008, re-irradiation to local recurrence has been performed. Because of their good physical and biological properties, carbon ions are excellent tools for re-irradiation to small recurrences. Special care must be taken to avoid toxicity of previously irradiated critical organs.

15.5.5.1 A Case with In-Field Recurrence

A 34-year-old man affected by ACC was treated with C-ion RT in January 2006. The nasal cavity and paranasal sinuses were almost entirely replaced by the tumor, which was distinctly seen on MET-PET. A total dose of 64 GyE was administered in 16 fractions over 4 weeks using three portals. At 24 months after C-ion RT, remarkable shrinkage of the tumor was observed (Fig. 15.19).

At 33 months after C-ion RT (Fig. 15.20), however, the patient developed a new lesion, seen within CTV2 on MRI and MET-PET. Biopsy indicated the same histology as the primary tumor. The lesion was judged to be an in-field recurrence, for which C-ion RT was again attempted, with 57.6 GyE in 12 fractions using three portals. At 42 months

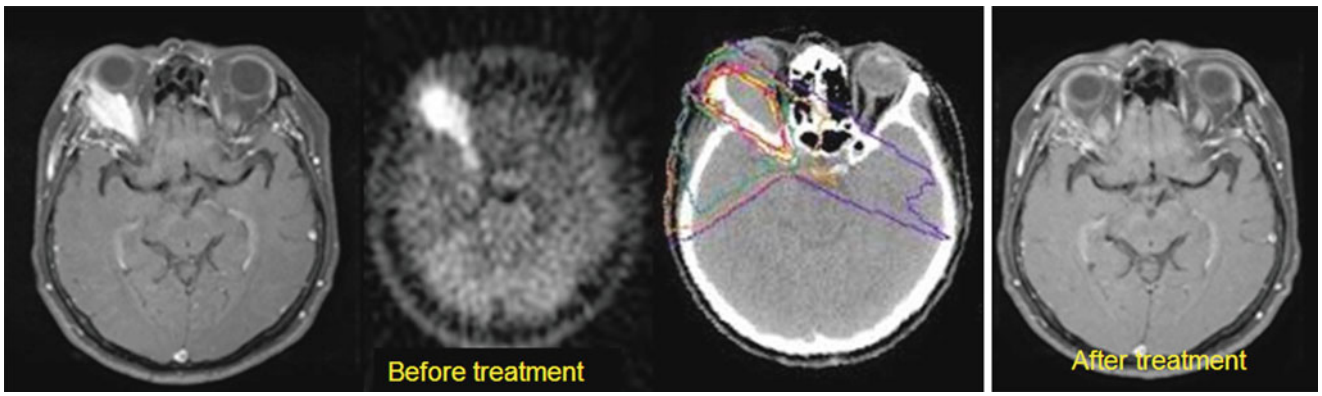

Fig. 15.21 Magnetic resonance and MET-PET images and isodose distribution. Isodose level: *red* = 96 %; *orange* = 90 %; *magenta* = 60 %; *green* = 50 %; *cyan* = 30 %; *light orange* = 20 %; *purple* = 10 %. Contour: *yellow* = clinical target volume

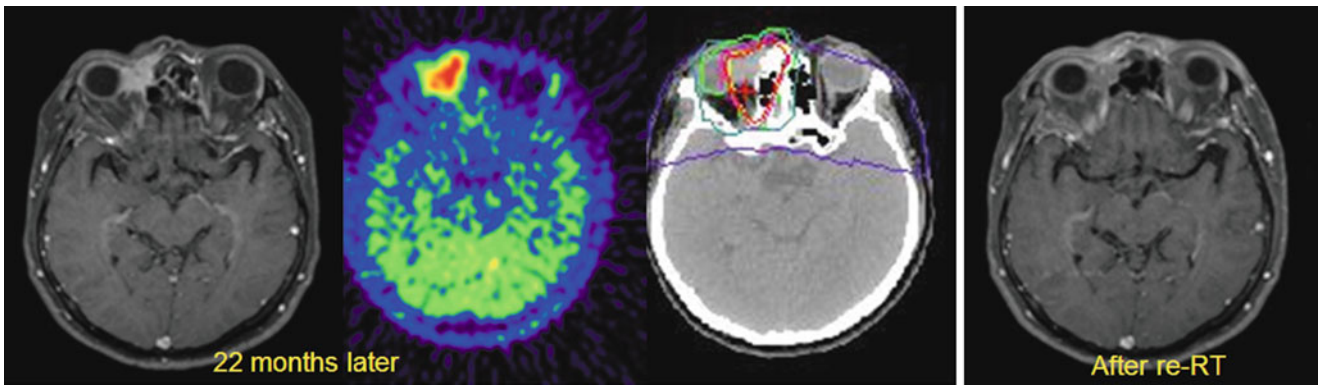

Fig. 15.22 Magnetic resonance and MET-PET images before and after re-irradiation and isodose distribution. Isodose level: *red* = 96 %; *orange* = 90 %; *magenta* = 70 %; *green* = 50 %; *cyan* = 30 %; *purple* = 10 %. Contour: *yellow* = clinical target volume

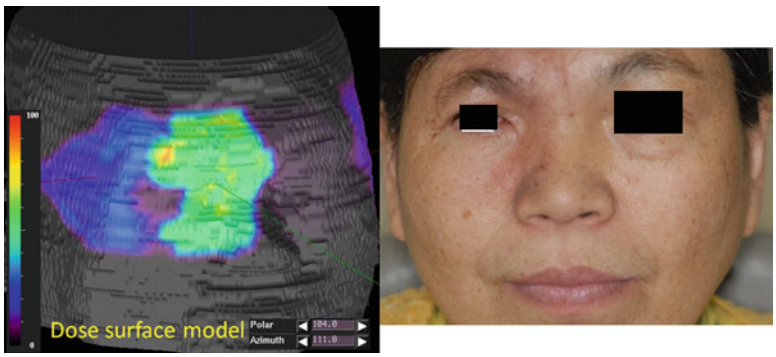

Fig. 15.23 Dose-surface model before re-irradiation and late skin reaction

after the initial C-ion RT (9 months after re-irradiation), the tumor disappeared completely without severe side effects.

15.5.5.2 A Case with Marginal Relapse

A 56-year-old woman had lacrimal gland ACC and was treated with C-ion RT in July 2005. MRI and MET- PET showed the presence of the tumor in the inner part of the orbital cavity. A total dose of 57.6 GyE was administered in 16 fractions over 4 weeks. The nasal part of the orbit was not irradiated. At 10 months after C-ion RT, complete response was achieved (Fig. 15.21).

Twenty-two months after C-ion RT (Fig. 15.22), recurrence was evident on MRI and MET-PET. The lesion originated in the nasal part of the orbit that had not received full dose and was considered as marginal recurrence within the CTV1. C-ion RT was performed again with 57.6 GyE in 12 fractions.

Four months after re-irradiation with carbon ions, a complete MET-PET and MRI response was achieved. Skin sparing is critical in re-irradiation. In this case, the use of multi-portals facilitated reduction of the high-dose area to a small spot. Skin reaction 1 week after re-irradiation was mild (G1) (Fig. 15.23).

References

1. Lengyel E, Gilde K, Remenár E, et al. Malignant mucosal melanoma of the head and neck. Pathol Oncol Res. 2003;9: 7–12.
2. Mendenhall WM, Morris CG, Amdur RJ, et al. Radiotherapy alone or combined with surgery for adenoid cystic carcinoma of the head and neck. Head Neck. 2004;26:154–62.
3. Mendenhall WM, Amdur RJ, Hinerman RW, et al. Head and neck mucosal melanoma. Am J Clin Oncol. 2005;28:626–30.
4. Bridger AG, Smee D, Baldwin, et al. Experience with mucosal melanoma of the nose and paranasal sinuses. ANZ J Surg. 2005;75:192–7.
5. Mendenhall WM, Morris CG, Amdur RJ, et al. Radiotherapy alone or combined with surgery for salivary gland carcinoma. Cancer. 2005;103:2544–50.
6. Krengli M, Masini L, Kaanders JH, et al. Radiotherapy in the treatment of mucosal melanoma of the upper aerodigestive tract; analysis of 74 cases. A Rare Cancer Network study. Int J Radiat Oncol Biol Phys. 2006;65:751–9.
7. Cheng YF, Lai CC, Ho CY, et al. Toward a better understanding of sinonasal mucosal melanoma: clinical review of 23 cases. J Chin Med Assoc. 2007;70:24–9.
8. Kanai T, Endo M, Minohara S, et al. Biophysical characteristics of HIMAC clinical irradiation system for heavy-ion radiation therapy. Int J Radiat Oncol Biol Phys. 1999;44:201–10.
9. Tsujii H, Morita S, Miyamoto T, et al. Preliminary results of phase I/II carbon-ion therapy at the National Institute of Radiological Sciences. J Brachytherapy Int. 1997;3:1–8.
10. Tsujii H, Mizoe JE, Kamada T, et al. Overview of clinical experiences on carbon ion radiotherapy at NIRS. Radiother Oncol. 2004;73:41–9.
11. Tsujii H, Mizoe J, Kamada T, et al. Clinical results of carbon ion radiotherapy at NIRS. J Radiat Res. 2007;48A:A1–13.
12. Mizoe J, Tsujii H, Kamada T, et al. Dose escalation study of carbon ion radiotherapy for locally advanced head-and-neck cancer. Int J Radiat Oncol Biol Phys. 2004;60:358–64.
13. Kanematsu N, Endo M, Futami Y, et al. Treatment planning for the layer-stacking irradiation system for three-dimensional conformal heavy-ion radiotherapy. Med Phys. 2002;29:2823–9.
14. Hasegawa A, Mizoe JE, Mizota A, et al. Outcomes of visual acuity in carbon ion radiotherapy: analysis of dose-volume histograms and prognostic factors. Int J Radiat Oncol Biol Phys. 2006;64:396–401.
15. Hirasawa N, Tsuji H, Ishikawa H, et al. Risk factors for neovascular glaucoma after carbon ion radiotherapy of choroidal melanoma using dose-volume histogram analysis. Int J Radiat Oncol Biol Phys. 2007;67:538–43.